Moderately strong vorticity in a bathtub-type flow

A.Y.Klimenko
Department of Mechanical Engineering
The University of Queensland, Qld 4072, Australia
Email: klimenko@mech.uq.edu.au

Abstract

Theoretical and numerical analysis is performed for an inviscid axisymmetric vortical bathtub-type flow. The level of vorticity is kept high so that the image of the flow on the radial-axial plane (r-z plane) is not potential. The most significant findings are: 1) the region of validity of the strong vortex approximation is separated from the drain by a buffer region; 2) the power-law asymptote of the stream function, specified by $\Delta\psi \sim r^{4/3}\Delta z$, appears near the axis when vorticity in the flow is sufficiently strong and 3) the local Rossby number in the region of $4/3$ power-law is not very sensitive to the changes of the initial vorticity level in the flow and the global Rossby number.

Published: Theoret. Comput. Fluid Dynamics (2001) 14: 243257

1 Introduction

The bathtub vortex is a phenomenon well-known even by nonspecialists: when water is drained from a large tank through a small orifice, the flow is composed of the combination of a translational motion towards the orifice and a rotational motion. The relative intensity of the rotation may vary significantly depending on the initial distribution of the vorticity within the fluid but the rotation never vanishes completely due to the Earth's rotation (Shapiro 1962). Simple observations of bathtub vortices indicate that 1) the core of the flow is axisymmetric, 2) the bulk of the flow usually remains laminar even if the Reynolds number is very large and 3) the flow seems steady (or quasi-steady). The relative intensity of rotation is characterized by the Rossby number (Rs). When the Rossby number is large, the vorticity is relatively weak and the flow image on the radial-axial (r-z) plane is potential (we use the term "potential" for the flows with negligibly small level of the circumferential vorticity ω_θ without expecting that the axial component of vorticity ω_z takes zero values). Determining characteristics of the potential flows is standard.

In the present work, we are interested in flows with smaller Rossby numbers and stronger vorticity when the r-z image of the flow is far from being potential. Einstein and Li (1951) investigated the case of asymptotically small Rossby numbers ($\mathrm{Rs} \to 0$). This approximation is referred to here as the strong vortex approximation. Lewellen (1962) applied the strong vortex asymptotic analysis to a steady strong vortex in a viscous fluid. Lundgren (1985) carried out a similar asymptotic analysis for a bathtub flow focusing on unsteady effects rather than on the global influence of viscosity. This publication is most relevant to the present work. Lundgren (1985) assumed that the Rossby number is so small that the strong vortex approximation is valid everywhere in the flow. The advantage of this solution is its relative simplicity but the strong vortex approximation does not comply with the conventional boundary conditions of zero radial velocity in the draining pipe. In addition, the flow above the draining pipe is determined by the axial velocity profile at the drain which remains unknown and was presumed by Lundgren (1985). It is not likely that this flow scheme corresponds to the bathtub flow observed in experiments. Klimenko (1998b) demonstrated that a sudden change in a strong vortex flow would cerate a buffer region near the disturbance. The strong vortex approximation is not valid in the buffer region. The experiments of Sakai, Madarame and Okamoto (1996) indicate that the axial velocity is a linear function of z (this behaviour corresponds to the strong vortex approximation) above the drain but not near the drain where the flow experiences rapid acceleration. Hence it is likely that, in a realistic bathtub flow, the strong vortex approximation may be valid in the bulk of the flow but not in the immediate vicinity of the drain.

It is well-known that the nonlinear interactions of vorticity and velocity are the most common sources of instability and turbulence in fluid flows. This problem is usually not accounted in inviscid flows since viscosity is generally responsible for the vorticity generation in boundary layers near the solid walls. In the bathtub-type flow, vorticity is inherently present in the flow and may, under certain conditions discussed in the paper, cause physical and numerical instabilities. It is possible, of course, to solve Navier-Stokes equations instead of equations governing inviscid evolution of vorticity and set the viscosity at a level which is sufficiently high for dampening all possible instabilities. The same effect can be achieved by introducing turbulent viscosity. Although this approach may generate some solutions, they are not much relevant to the bathtub vortex flow where the Reynolds number is, typically, very high. The bulk of the vortex flow is laminar and effectively inviscid. The viscous effects remain local and may be significant only near the walls or near the axis as considered by Lewellen (1962). Obtaining solutions of equations governing inviscid evolution of vorticity, which is the focus of the present work, represents a demanding numerical problem.

When considering a bathtub-type vortical flow, some researches take into account the air dip formed at the surface (Lundgren 1985, Forbes and Hocking 1994) while others tend to neglect it (Lewellen 1962, Marris 1967). For the asymptotic limit of the fast rotation, determining the shape of the air dip can be done analytically (Lundgren 1985). When vorticity is weak and the flow is potential, the shape of the air dip can be found numerically (Forbes and Hocking 1994). For the flows with moderately strong vorticity, which are considered in the present work, the analysis of the free surface shape is not computationally feasible.

The bathtub flow is characterized by slow evolution of the flow. This property is used here to obtain quasi-steady solutions. However, the bathtub flow can not be treated as completely steady: the circulation γ in the near-axis region gradually increases as the fluid particles arrive from peripheral regions where the initial value of γ is greater. The main difference between the terms "quasi-steady flow" and "steady flow" is that the equations describing steady axisymmetric flows of an inviscid fluid is not applicable to the bathtub vortex. In a steady flow, the lines of constant γ must coincide with the streamlines and this is certainly not valid for a bathtub-type vortical flows. In general, the axisymmetric steady flows allow for analytical integration of the vorticity ω_θ which would significantly simplify the calculations (Long 1953, Batchelor 1967).

2 The governing equations

A general axisymmetric inviscid flow with vorticity is governed by the following set of equations (Batchelor 1967)

$$\frac{\partial^2\psi}{\partial z^2}+r\frac{\partial}{\partial r}\left(\frac{1}{r}\frac{\partial\psi}{\partial r}\right)=-r\omega_\theta \tag{1}$$

$$v_z=\frac{1}{r}\frac{\partial\psi}{\partial r},\qquad v_r=-\frac{1}{r}\frac{\partial\psi}{\partial z} \tag{2}$$

$$\omega_\theta=\frac{\partial v_r}{\partial z}-\frac{\partial v_z}{\partial r};\quad \omega_r=-\frac{\partial v_\theta}{\partial z}=-\frac{1}{r}\frac{\partial\gamma}{\partial z};\quad \omega_z=\frac{1}{r}\frac{\partial v_\theta r}{\partial r}=\frac{1}{r}\frac{\partial\gamma}{\partial r} \tag{3}$$

$$\frac{d\gamma}{dt}=0 \tag{4}$$

$$\frac{d\omega_\theta/r}{dt}=\gamma\boldsymbol{\omega}\cdot\boldsymbol{\nabla}r^{-2}=-2\frac{\gamma\omega_r}{r^3}=\frac{1}{r^4}\frac{\partial\gamma^2}{\partial z} \tag{5}$$

where

$$\frac{d}{dt}\equiv\frac{\partial}{\partial t}+v_z\frac{\partial}{\partial z}+v_r\frac{\partial}{\partial r} \tag{6}$$

represents the substantial derivative; r, z and θ are radial, axial and circumferential coordinates; ψ is the stream function; v_r, v_z, v_θ are the velocity components; $\gamma\equiv v_\theta r$ is the circulation; ω_r, ω_z, ω_θ are the vorticity components. Equation (5) controls generation of the vorticity component ω_θ.

If the flow is steady, then the streamlines $\psi=\text{const}$ coincide with the lines of $\gamma=\text{const}$ and equation (5) can be integrated (Batchelor 1967)

$$\omega_\theta r=\gamma\frac{\partial\gamma}{\partial\psi}-r^2\frac{\partial B}{\partial\psi} \tag{7}$$

where $B\equiv\mathbf{v}^2/2+p/\rho$ is the Bernoulli integral. In this flow, γ and B can be expressed as functions of ψ since these values are constant along streamlines.

If the vorticity in the flow is strong, the leading order approximation of the stream function is given by Einstein and Li (1951)

$$\psi=f_0(r,t)+f_1(r,t)\,z \tag{8}$$

where f_0 and f_1 are arbitrary functions. As determined by equation (8), the radial velocity v_r does not depend on z and the axial velocity v_z is the linear function of z. Generally, the strong vortex approximation is not consistent with (7).

3 The flow in a bathtub

A cylindrical tub of radius r_b is drained though the pipe of radius r_d which is assumed to be much smaller than r_b (see Figure 1). Before draining is started at $t = 0$, the flow is represented by the solid-body rotation with the constant vorticity $\omega_z = \omega_0$, $\omega_r = 0$ and $\omega_\theta = 0$. The level of the water in the tub is given by $h = h(t)$ and $h_0 = h(0)$ is its initial value. The draining speed is determined by $u \equiv -dh/dt$ and $q \equiv ur_b^2/2$ is introduced so that $2\pi q$ represents the volume flow rate.

3.1 Peripheral flow

In the bulk of the tub, the flow is given by

$$\psi = \frac{1}{2}u\left(r_b^2 - r^2\right)\frac{z}{h}, \qquad v_r = \frac{1}{2}\frac{u}{h}\left(r - \frac{r_b^2}{r}\right), \qquad v_z = -\frac{u}{h}z \tag{9}$$

While evolution of the circulation and vorticity that corresponds to the specified initial conditions and the velocity field is represented by

$$\gamma\left(t\right) = \frac{\omega_0}{2}\left(r_b^2 - r_b^2 H + r^2 H\right), \;\; \omega_z = H\omega_0, \;\; \omega_r = 0, \;\; \omega_\theta = 0 \tag{10}$$

where $H \equiv h/h_0$. The velocity field given by (9) satisfies equations (1)-(5) as well as the boundary conditions $v_r = 0$ at $r = r_b$; $v_z = -u$ at $z = h$ and $v_z = 0$ at $z = 0$. However, this representation of the velocity is, obviously, not valid near the drain. The flow determined by (9) and (10) is potential ($\omega_\theta = 0$) and, at the same time, this flow complies with the strong vortex approximation (8). The flow specified by (9) and (10) is not steady. The applicability of equations (9) and (10) is determined by their ability to match the flow near the axis. Obviously, this solution is valid when the water is shallow $h \ll r_b$. Since equations (9) and (10) represent the strong vortex approximation, the solution should be also valid when the global Rossby number $\mathrm{Rs}_b \equiv u/(r_b\omega_0)$ is small. The most interesting feature of the flow specified by (10) is that γ increases while ω_z does not increase with time. This indicates a singularity forming near the axis which is actually perceived as the bathtub vortex.

If the water is sufficiently deep, Rs_b is sufficiently large and the flow rate is constant, then, after a short initial period of time this flow is similar to the flow in a sudden pipe contraction and can be treated as steady. The steady flow is governed by equations (1) and (7). As rotation speed increases and Rs_b decreases, the vorticity ω_θ becomes more and more significant. Batchelor (1967) demonstrated that as soon as Rs_b^2 reaches $\sim 1/3.8$, the flow loses its ability to adjust itself to small changes of the tub radius, r_b. It is likely that at this point the structure of the flow is changed so that (1) and (7) do not control the flow. One possible scenario is the appearance of recirculation zones, loss of stability and transition to turbulence. Another scenario, which is considered here, is development of the unsteady vortical flow specified by equations (9) and (10). Klimenko (1998b) found that, in the steady flow, rotation may be noticeable near the drain but it does not have characteristic features of the bathtub vortex. Steady flow is not of much interest for the present work.

The leading terms of the near-axis asymptote of the flow specified by (9) and (10) are given by

$$\psi_0 = \frac{q}{h}z, \quad v_{r0} = -\frac{q}{h}\frac{1}{r}, \quad v_{z0} = 0, \quad \omega_{z0} = H\omega_0, \quad \gamma_0 = \frac{\omega_0}{2}r_b^2\left(1 - H\right) \tag{11}$$

It should be noted that the approximation for γ is not applicable during a very short initial period when $H \approx 1$. This short period is not considered in the present work. Although the Strouhal number calculated for the flow specified by (11) appears to be small, this flow is not steady since the velocity is directed towards the flow axis, while direction of vorticity is vertical. Equations (11) set the inflow boundary conditions for the near-axis region.

3.2 The near-axis region

In the region surrounding the axis, the flow specifications given by (9) are, obviously, not applicable. The near-axis flow, which can not be represented by analytical formulae, is the actual subject of the present study. We rewrite the system of equations (1) - (5) in the dimensionless form:

$$L_d^2 \frac{\partial^2 \Psi}{\partial Z^2} + R \frac{\partial}{\partial R} \left(\frac{1}{R} \frac{\partial \Psi}{\partial R} \right) = -R\Omega_\theta \tag{12}$$

$$V_z = \frac{1}{R} \frac{\partial \Psi}{\partial R}, \qquad V_r = -\frac{1}{R} \frac{\partial \Psi}{\partial Z} \tag{13}$$

$$\Omega_\theta = \frac{\partial V_r}{\partial Z} - \frac{\partial V_z}{\partial R}; \quad \Omega_r = -\frac{\partial V_\theta}{\partial Z} = -\frac{1}{R} \frac{\partial \Gamma}{\partial Z}; \quad \Omega_z = \frac{1}{R} \frac{\partial V_\theta R}{\partial R} = \frac{1}{R} \frac{\partial \Gamma}{\partial R} \tag{14}$$

$$\frac{d\Gamma}{dT} = 0 \tag{15}$$

$$\frac{d\Omega_\theta / R}{dT} = -\frac{2}{\mathrm{Rs}_d} \frac{\Gamma \Omega_r}{R^3} \tag{16}$$

where

$$\frac{d}{dT} \equiv \mathrm{St}_d \frac{\partial}{\partial T} + V_z \frac{\partial}{\partial Z} + V_r \frac{\partial}{\partial R}, \tag{17}$$

$$\mathrm{Rs}_d \equiv \frac{q/r_d^2}{(\gamma_0 \omega_{z0})^{1/2}} = \mathrm{Rs}_b \left(\frac{r_b}{r_d} \right)^2 [H(1-H)]^{-1/2} \tag{18}$$

$$\mathrm{St}_d \equiv \frac{\omega_{z0} r_d^2}{\gamma_0} = 2 \left(\frac{r_d}{r_b} \right)^2 \left(\frac{H}{1-H} \right), \quad L_d \equiv \frac{r_d}{h} \tag{19}$$

represent the Rossby number, the Strouhal number and the geometric parameter of the near-axis region; the normalized values are denoted by capital letters:

$$R = \frac{r}{r_d}, \quad Z = \frac{z}{h}, \quad \Psi = \frac{\psi}{q}, \quad V_r = v_r \frac{r_d h}{q}, \quad V_z = v_z \frac{r_d^2}{q}, \tag{20}$$

$$T = t \frac{\omega_{z0} q}{\gamma_0 h}, \quad \Omega_\theta = \omega_\theta \frac{r_d^3}{q}, \quad \Gamma = \frac{\gamma}{\gamma_0}, \quad \Omega_z = \frac{\omega_z}{\omega_{z0}}, \quad \Omega_r = \frac{\omega_r}{\omega_{z0}} \frac{h}{r_d} \tag{21}$$

The typical values are selected on the basis of the near-axis asymptote of the peripheral flow (11) taken at a chosen time moment, say $t = t_1$. In the near-axis region the Rossby number Rs_d is much larger than the Rossby number Rs_b and the Strouhal number is very small except for a very short initial period. We seek quasi-steady solutions of this system of equations in form of the expansions $\Gamma = \Gamma_0 + \mathrm{St}\, \Gamma_1 + ...$, $\Psi = \Psi_0 + ...$, etc. With the exception of the circulation Γ, which needs two terms in the expansion, only the leading order terms are needed for the present analysis. The subscripts "0" denoting the leading terms is omitted (except for Γ). Most of equations (12) – (16) remain without changes, while the equations involving Γ take the form

$$\Omega_r = -\frac{1}{R}\frac{\partial \Gamma_1}{\partial Z}, \quad \Omega_z = \frac{1}{R}\frac{\partial \Gamma_1}{\partial R} \tag{22}$$

$$V_z \frac{\partial \Gamma_0}{\partial Z} + V_r \frac{\partial \Gamma_0}{\partial R} = 0, \qquad V_z \frac{\partial \Gamma_1}{\partial Z} + V_r \frac{\partial \Gamma_1}{\partial R} = -\frac{\partial \Gamma_0}{\partial T} \tag{23}$$

$$V_z \frac{\partial \Omega_\theta / R}{\partial Z} + V_r \frac{\partial \Omega_\theta / R}{\partial R} = -\frac{2\Gamma_0}{\mathrm{Rs}_d}\frac{\Omega_r}{R^3} \tag{24}$$

The boundary conditions for Γ, Ψ and Ω_θ are now considered. For the near-axis region, the upstream conditions are determined by matching the variables of the near axis region with (11) for $t = t_1$

$$\Gamma_0 \to 1, \;\; \Gamma_1 \to \frac{1}{2}R^2 + (\Gamma_1)_0, \;\; \Psi \to Z, \;\; \Omega_\theta \to 0 \quad \text{as} \quad R \to \infty \tag{25}$$

Note that $\Omega_z \to 1$ upstream from the near-axis region. The constant $(\Gamma_1)_0$ does not affect calculations and, without loss of generality, can be set to zero at the upstream boundary of the computational domain. As it can be inferred from equation (23), the leading order circulation remains constant. The slow time T is chosen so that the time derivative of the circulation equals to unity. Thus we have

$$\Gamma_0 = 1, \;\; \frac{\partial \Gamma_0}{\partial T} = \frac{h}{\omega_{z0} q}\frac{\partial \gamma_0}{\partial t} = 1 \tag{26}$$

at $t = t_1$ in the whole near-axis region. The computational domain and the boundary conditions used are shown in Figure 2. It should be emphasized that the conventional boundary conditions $\partial\Psi/\partial Z = 0$ are applied at the boundary $Z = -H_d$ in the drain.

4 The main features of bathtub-type vortical flows

In this section we analyze the features of inviscid bathtub-type vortical flows which are important for understanding of the results of computations. In our considerations we repeatedly use the fact that, in inviscid fluid, the vorticity vectors $\boldsymbol{\omega}$ evolve in exactly the same way as the corresponding material line elements (Batchelor 1967).

Proposition 1 *Positive values of the product $\omega_z \gamma$ have a stabilizing effect on the flow while negative values of the product $\omega_z \gamma$ would have a destabilizing effect.*

Let us assume that, initially, the vorticity vector and the corresponding material line element (or material vector) $\mathrm{A}_0\mathrm{B}_0$ shown in Figure 3 are directed along z-axis ($\omega_r = 0$). Since $\partial\gamma/\partial z = 0$, the value of γ must be the same at A_0 and B_0. After a short time interval, the position of the same material line element in a bathtub-type flow without significant vorticity is shown by $\mathrm{A}_1\mathrm{B}_1$. The vorticity component ω_r takes a negative value. Since $r(\mathrm{A}_1) > r(\mathrm{B}_1)$, the rotation at B_1 is faster. If γ has the same sign as ω_z (negative in Figure 3) then the vector $\mathrm{A}_1\mathrm{B}_1$ has its θ-component directed towards the reader. Hence, the flow generates the vorticity ω_θ whose direction is shown in Figure 3. This vorticity acts to rotate the vector $\mathrm{A}_1\mathrm{B}_1$ back to the vertical direction. If $|\gamma|$ is large, a small deviation from the vertical direction, such as shown by the vector $\mathrm{A}_1\mathrm{B}_1'$, would be sufficient to generate the vorticity ω_θ required to preserve the initial direction of the vector $\mathrm{A}_0\mathrm{B}_0$. In this case, the vorticity/velocity interactions adjust the flow in a way which keeps generation of ω_θ under control. Thus, the fast rotation in a vortex-type flow has some stabilizing effect provided $\gamma\omega_z > 0$. This condition is essentially the same as the well-known Rayleigh condition for stability of the inviscid flow between rotating cylinders (Vanyo 1993). A negative value of the product $\gamma\omega_z$ would have an opposite, destabilizing effect on the flow.

Proposition 2 *The bathtub vortical flow can not be transformed in the drain into a vertical pipe flow with $v_r = 0$. The flow in the draining pipe would continue to evolve. The characteristic length of this evolution is given by $\Delta z = h\mathrm{Rs}_d^2$.*

Indeed, let us assume that $v_r = 0$ downstream from the drain orifice. Evolution of vorticity is similar to evolution of the material vector $\mathrm{A}_0\mathrm{B}_0$. In a quasi-steady flow, the fluid particles A and B move along streamlines (see Figure 3). The time-shifted position of the vector $\mathrm{A}_0\mathrm{B}_0$ is shown by the vector $\mathrm{A}_2\mathrm{B}_2$, which has a non-zero radial component denoted as $\mathrm{A}_2\mathrm{B}_{2r}$ in Figure 3. Hence, $\omega_r \neq 0$ in the drain. As it follows from equation (5), $d\omega_\theta/dt \neq 0$ and the flow continues to evolve: $\partial v_z/\partial z \neq 0$. The continuity equation

$$\frac{\partial v_z}{\partial z} + \frac{1}{r}\frac{\partial}{\partial r}(rv_r) = 0 \tag{27}$$

requires that $v_r \neq 0$. The assumption $v_r = 0$ is not valid.

Considering that $|\mathrm{A}_0\mathrm{B}_0|/h \sim |\mathrm{A}_2\mathrm{B}_{2r}|/r_d$, we infer that the radial component of vorticity in the drain can be estimated by $\omega_r \sim \omega_{z0} r_d/h$. The circumferential vorticity can achieve a significant change $\omega_\theta \sim v_z/r_d$ of its value within the distance $\Delta z \sim r_d^2 v_z \omega_\theta/(\gamma_0\omega_r)$. By combining these equations with obvious $q \sim v_z r_d^2$, we obtain $\Delta z \sim h\mathrm{Rs}_d^2$.

Practically, the development of the flow in the drain can be neglected provided $\Delta z \gg r_d$. This leads us to the following inequality for the Rossby number Rs_r which is calculated on the basis of the radial vorticity component ω_r

$$\mathrm{Rs}_r^2 \equiv \frac{v_z^2}{\gamma_0\omega_r} \sim \mathrm{Rs}_d^2/L_d \gg 1 \tag{28}$$

If this condition in not valid, it is likely that intense increase of the vorticity ω_θ in the flow would cause appearance of recirculation zones. If this condition is valid then ω_r can be neglected and the flow in the drain (but not in the tub) can be approximately treated as steady, since both velocity and vorticity have vertical direction.

Proposition 3 *A quasi-steady bathtub-type vortical flow can not have any recirculation zones.*

Indeed, in a flow with recirculation zones, some of the streamlines would form a closed path. According to equations (23) and (26), the value of Γ_1 monotonically decreases along streamlines and this is impossible when a streamline forms a closed path. In addition, the sign of the derivative $\partial\Gamma_1/\partial Z$ is likely to change within a recirculation zone and this would violate the stability condition $\omega_z\gamma > 0$.

Proposition 4 *If the stream function and the circulation of a quasi-steady bathtub-type vortical flow remain uniformly smooth within a fixed region as the local Rossby number tends to zero, then $\omega_r/\omega_z \to 0$ and the strong vortex approximation is valid in this region.*

Since the stream function is uniformly smooth in the region, the absolute values of the derivatives of the stream function are restricted and the velocity components can be estimated $rv_z \lesssim \Delta\psi/\Delta r$ and $rv_r \lesssim \Delta\psi/\Delta z$ where $\Delta\psi$ is the change of ψ in the region whose size is denoted by Δr and Δz. We introduce $v = (v_z^2 + v_r^2)^{1/2}$ and $l_m = \min(\Delta r, \Delta z)$ and estimate $rv \lesssim \Delta\psi/l_m$. Equation (1) restricts the values of circumferential vorticity $r|\omega_\theta| \lesssim \Delta\psi/l_m^2$. Equation (5), which specifies the change of circumferential vorticity in the region, yields

$$\Delta(\omega_\theta/r) = -2\int \frac{\omega_r\gamma_0}{vr^3}dl \gtrsim \frac{l_m\gamma_0}{\Delta\psi}\int \frac{\omega_r}{r^2}dl$$

where the integrals are evaluated along a section of a chosen streamline laying within the region. Since ψ is uniformly smooth in region, we can select a characteristic radius for a chosen streamline.

The following estimation of the integral takes into account that ω_r must be smooth and does not oscillate in the region. Combining the inequalities obtained for ω_θ gives $(\Delta\psi)^2 \gtrsim l_m^4 \gamma_0 \omega_r$ or $\beta l_m^2/r^2 \lesssim \mathrm{Rs}^2$ where

$$\mathrm{Rs}^2 \equiv \frac{v^2}{\omega_z \gamma_0} \tag{29}$$

is the Rossby number and $\beta \equiv \omega_r/\omega_z$. Considering that the region is fixed, we obtain $\beta \to 0$ as $\mathrm{Rs}^2 \to 0$. This estimation requires that $\gamma \to \gamma(r)$ and $v_r \to v_r(r)$ as determined by equations (3) and (2). The stream function which keeps $v_r = v_r(r)$ is given by (8). This proves the proposition. The applicability of the strong vortex approximation in different parts of the flow is determined by condition $\mathrm{Rs} \ll 1$, where the Rossby number given by (29) is evaluated locally and depends on local values of v and ω_z. The order of the local Rossby number does not necessarily coincide with the order of Rs_d – the global Rossby number of the whole near-axis region.

Proposition 5 *The flow field specified by the strong vortex approximation can not satisfy the boundary conditions in the drain* $\partial\psi/\partial z = 0$ *and also can not be adjusted in a thin layer in order to satisfy these conditions.*

Indeed, the boundary conditions in the drain $\partial\psi/\partial z = 0$ require that $f_1 = 0$ in (8). Hence, v_r must be zero in the whole region above the drain which is physically impossible.

If the strong vortex approximation can not satisfy the conditions in the drain, the flow may be adjusted in a layer which is asymptotically thin for small values of the Rossby number. Within this layer, the strong vortex approximation is not valid. Physically, this layer may be located on the surface OO´(see Figure 2) or on any other surface separating the tub and the drain. Mathematically, this layer can also appear at $Z = -H_d$ where the drain boundary conditions are applied. For simplicity, we will consider only horizontal layers and demonstrate that, in these layers, the flow can not be adjusted to satisfy the boundary conditions in the drain. First, we note the evolution of vorticity equations

$$\frac{d\omega_z}{dt} = \omega_z \frac{\partial v_z}{\partial z} + \omega_r \frac{\partial v_z}{\partial r}, \quad \frac{d\omega_r}{dt} = \omega_z \frac{\partial v_r}{\partial z} + \omega_r \frac{\partial v_r}{\partial r} \tag{30}$$

where d/dt is determined by (6), can be formally obtained from (4), (3) and (27). The strong vortex approximation can not satisfy $v_r = 0$. Within the thin layer (or thin boundary layer if the layer is located at $Z = -H_d$) the variables are marked by superscript "$\circ$" to distinguish them from the outer flow. Using $z^\circ = (z - h_d)/\delta$ and taking into account (3), (4), (5), (27) and (30), we obtain the following leading order equations

$$\frac{\partial v_z^\circ}{\partial z^\circ} = 0, \;\; \frac{\partial \omega_z^\circ}{\partial z^\circ} = 0, \;\; \frac{\partial \gamma^\circ}{\partial z^\circ} = 0 \implies v_z^\circ = v_z, \;\; \omega_z^\circ = \omega_z, \;\; \gamma^\circ = \gamma$$

$$\omega_\theta^\circ = \frac{1}{\delta}\frac{\partial v_r^\circ}{\partial z^\circ} + \omega_\theta, \;\; v_z \frac{\partial \omega_r^\circ}{\partial z^\circ} = \omega_z \frac{\partial v_r^\circ}{\partial z^\circ}, \;\; v_z \frac{\partial \omega_\theta^\circ}{\partial z^\circ} = -2\delta \frac{\gamma \omega_r^\circ}{r^2}$$

Elementary transformations of the equations in the second line yield

$$\frac{\partial^2 \omega_r^\circ}{\partial (z^\circ)^2} + \frac{\delta^2}{r^2}\frac{2}{\mathrm{Rs}_z^2}\omega_r^\circ = 0, \quad v_r^\circ = \frac{v_z}{\omega_z}\omega_r^\circ + c_v, \quad \mathrm{Rs}_z^2 \equiv \frac{v_z^2}{\gamma \omega_z} \tag{31}$$

where c_v is a constant which is determined by the upstream conditions. We consider Rs_z as a local value which can be calculated at different physical locations. The local Rossby number should be distinguished from the global parameters of the flow Rs_b and Rs_d. Equation (31) determines that, when Rs_z is small, rapid changes are indeed possible within a thin layer. The thickness of the layer can be defined as $\delta = r\mathrm{Rs}_z$. However, the solution of (31) is given by a propagating wave $\omega_r^\circ = c\cos(2z/(r\mathrm{Rs}_z))$ which can not simultaneously satisfy the upstream conditions $v_r \neq 0$, $\omega_r \to 0$ specified by the strong vortex approximation and the downstream condition $v_r = 0$. Physically, this indicates that, when Rs_z is small, the disturbances from the boundary conditions in the drain tend to propagate upstream and affect the whole flow. These waves bear some resemblance to the Kelvin inertial waves in uniformly rotating fluids (Greenspan 1968). The intensity of generated vorticity which can be estimated by $\omega_\theta \sim v_r/\mathrm{Rs}_z$ is asymptotically high as $\mathrm{Rs}_z \to 0$. This indicates that the flow is likely to loose stability and become turbulent .

This consideration explains the conditions imposed on the flow in Proposition 4. Near the axis, the values of Rs and Rs_z defined in (29) and (31) are very similar. If the size of the region is asymptotically small or the flow in the region is not smooth, the strong vortex approximation may not be applicable since the solution of equation (31) does not comply with the strong vortex approximation. However, if Rs_z is small and the streamlines are smooth in a region, whose typical scale Δz is much greater than $\delta = r\mathrm{Rs}_z$ (that is $\Delta z^\circ >> 1$), then equation (31) takes the form $\omega_r = 0$ which is consistent with Proposition 4. Batchelor (1967) considered a steady axisymmetric vortical pipe flow and found that, if Rs_z is smaller than a certain critical number, the flow losses its ability to adjust itself to varying boundary conditions.

Proposition 6 *Assuming that the level of vorticity in a quasi-steady bathtub-type flow is sufficiently high and the power-law approximation $\Delta\Psi = C_1 R^\alpha \Delta Z$ of the stream function (where $\Delta Z \equiv 1 - Z$ and $\Delta\Psi \equiv 1 - \Psi$) is valid in a significant section of the near-axis region, the value of the exponent in this region is given by*

$$\alpha = 4/3 \tag{32}$$

The velocity components are determined by equation (13): $V_r = -C_1 R^{\alpha-1}$, $V_z = -C_1\alpha R^{\alpha-2}\Delta Z$. Since in the strong vortex flow we have $\Omega_r = 0$, equations (22), (23) and (26) yield $\Omega_z = -1/(V_r R)$. Combining equations for V_r, V_z and Ω_z determines the local Rossby number calculated on the basis of axial velocity

$$\mathrm{Rs}_z^2 = \frac{V_z^2}{\Gamma_0 \Omega_z}\,\mathrm{Rs}_d^2 = C_1^3\alpha^2\Delta Z^2 R^{3\alpha-4}\,\mathrm{Rs}_d^2 \tag{33}$$

Obviously, if the level of vorticity is very low, then the flow must be potential ($\omega_\theta = 0$) and $\alpha = 2$ near the axis. We assume now that vorticity is sufficiently strong to affect the flow somewhere at $R \approx R_1$. If $\alpha < 4/3$, then according to Equation (33), the value of Rs_z would be large for $R \ll R_1$ and the flow would become effectively potential. In a potential flow, $\alpha = 2$ and this value is in contradiction with $\alpha < 4/3$. If $\alpha > 4/3$, then the value of Rs_z would be very small at smaller radii ($R \ll R_1$). The streamlines of this flow should comply with the strong vortex approximation. According to the analysis of Proposition 5, this flow would not be able to satisfy the conditions in the drain. Hence α must be 4/3.

Since the local Rossby number Rs_z can not be very large or very small in the region of $\alpha = 4/3$, we can estimate $\mathrm{Rs}_z \sim 1$. The approximate character of this estimation should be emphasized. The substitution of $\mathrm{Rs}_z \sim 1$, $\alpha = 4/3$ and $\Delta Z \sim 1$ into (33) yields

$$C_1 \sim \left(\frac{\mathrm{Rs}_z}{\mathrm{Rs}_d}\right)^{2/3} \sim \mathrm{Rs}_d^{-2/3} \tag{34}$$

The axial component of the velocity $V_z \sim R^{-2/3}\Delta Z$ has a singularity at the axis. Physically, of course, the velocity can not tend to infinity. When the Reynolds number is high but not infinite, a thin viscous core is formed in the immediate vicinity of the axis as considered by Lundgren (1985). The singularity of $\alpha = 4/3$ disappears in the viscous core. Alternatively, an air core can be formed at the axis of the bathtub flow.

Proposition 7 *If the vorticity in the flow is sufficiently strong and the water is sufficiently deep so that the 4/3 power-law region extends up to the peripheral region of the flow, the transition between these regions occurs at*

$$R_1 \sim \mathrm{Rs}_d^{1/2} \tag{35}$$

The stream function in the region of $\alpha = 4/3$ is given by $\Delta\Psi = C_1 R^{4/3} \Delta Z$ while $\Delta\Psi = \Delta Z$ in the peripheral region. At $R \sim R_1$, these two representations of the stream function should match $C_1 R^{4/3} \Delta Z \sim \Delta Z$. After taking into account (34), we obtain (35). Of course, R_1 can not exceed the extend of the near-axis region of a potential flow specified by $r \sim h$ or $R \sim 1/L_d$. If $R_1 \gg 1/L_d$, then vorticity in the flow is weak and the intermediate region of $\alpha = 2$ appears. The division of the flow into the peripheral and near-axis regions suggests that at least one of the parameters $r_1 \equiv R_1 r_d$ or h must be much smaller than r_b. Since $\mathrm{Rs}_d \sim \mathrm{Rs}_b (r_b/r_d)^2$, the condition $r_1 \ll r_b$ takes the form $\mathrm{Rs}_b \ll 1$.

5 Numerical method

The flow in the near-axis region is analyzed numerically by seeking solution of the system of equations (12), (13), (22), (23) and (24) while taking into account (26). This system is effectively a non-linear integro-differential system of equations. Calculations are carried out on a regular grid with gradually varying steps and maximal resolution near the orifice. The calculations involve the following chain

$$\Psi_{\mathrm{old}} \overset{\mathrm{I}}{\Longrightarrow} (V_z, V_r) \underset{\Delta t,\ (\Gamma_1)_{\mathrm{old}}}{\overset{\mathrm{II}}{\Longrightarrow}} \Gamma_1 \overset{\mathrm{III}}{\Longrightarrow} \Omega_r \underset{\Delta t,\ (\Omega_\theta)_{\mathrm{old}}}{\overset{\mathrm{IV}}{\Longrightarrow}} \Omega_{\theta 1} \overset{\mathrm{V}}{\Longrightarrow} \Psi_{\mathrm{new}} \tag{36}$$

where equation (13) is used in step I, (23) and (26) in II, (22) in III, (24) and (26) in IV, (12) in V. Steps II, IV and V need boundary conditions. The boundary conditions used are shown in Figure 2. Although only quasi-steady solutions are sought, the time derivative is formally included into the substantial derivative as it is determined by equation (17). This allows to reach the quasi-steady solution by performing steps in time. The old values of Γ_1 and Ω_θ are needed only for time steps. The equations are discretized using second order finite-difference schemes. The choice for steps II and IV was made in favour of the upwinding scheme. When time evolution is used to reach convergence, the time derivatives are approximated by the first order implicit finite difference scheme. The operation defined by (36) is denoted in the rest of the paper as $\Psi_{\mathrm{new}} = \Lambda_{\Delta t}[\Psi_{\mathrm{old}}, (\Gamma_1)_{\mathrm{old}}, (\Omega_\theta)_{\mathrm{old}}]$ where Δt specifies the duration of the time steps. If no time evolution considered ($\Delta t = \infty$), then this operation is denoted as $\Psi_{\mathrm{new}} = \Lambda[\Psi_{\mathrm{old}}]$.

The calculations comprise several stages. First, the functional $F_\Lambda(\Psi) \equiv \|\Psi - \Lambda[\Psi]\|$, where the norm $\|\mathbf{a}\|$ of a vector $\mathbf{a}$ is introduced as $\left(\sum_i a_i a_i\right)^{1/2}$ and the sum is taken over values in each node of the computational domain, is minimized by the Levenberg-Marquardt algorithm. The minimization is performed on several progressively more refined grids. The best resolution is reached on a 51×37 grid. If the initial Ψ is set for a refined grid without taking into account Ψ obtained on coarser grid, the algorithm is not able to minimize F_Λ. Final convergence is achieved by ~ 30000 implicit small time steps. The calculations are terminated when the residual $F_\Lambda(\Psi)/\|\Psi\|$ reached $\sim 10^{-10}$. Practically, this means that the results presented here are exact solutions of the finite difference equations. The precision of the finite difference approximation is checked by recalculating Ψ on the 101×73 grid without attempting to reach the solution on this grid. The residual $F_\Lambda(\Psi)/\|\Psi\|$ calculated on a 101×73 grid is less then 1% in most of the calculations presented here.

The convergence of the time steps indicates stability of the solutions obtained. Overall physical stability at high Reynolds numbers is the remarkable property of the bathtub vortical flow

(Proposition 1). In numerical calculations, this stability is, however, quite fragile. Any, even small, disturbance may potentially cause rapid development of instabilities. If the initial conditions for Ψ are set well (for example, by using Ψ calculated on coarser grid), plausible time steps can be performed for quite a long time until a recirculation zone appears (usually, near the drain or near the axis). As soon as the recirculation zone appears, instabilities develop and the numerical approximation of the flow is rapidly destroyed. This behaviour is in agreement with the properties of the flow specified by Propositions 1 and 3. Unlike scalar transport (Klimenko 1998a), the vorticity transport involves nonlinear interactions of velocity and vorticity in an inviscid fluid (although these interactions are limited here by the axisymmetric conditions) which can be physically unstable. The initial minimization of the functional $F_\Lambda(\Psi)$ was absolutely necessary to obtain good initial conditions for convergence by time steps. This minimization, performed in the nearly 2000-dimensional space of the values of Ψ in each node, required substantial computational resources and this makes any further refinement of the grid (or significant enlarging of the computational domain) quite difficult. As it is noted above, the success of the minimization procedure is also dependent on the choice of a good initial approximation for Ψ. Generally it is more difficult to achieve convergence for smaller values of the Rossby number. Both the functional minimization procedure and the time steps often need a manual control over convergence. No convergence was reached for the values of Rs_d significantly smaller than these presented in the next section.

6 Results of the simulations

In a strong vortex flow, the axial component of velocity V_z is a linear function of Z as defined by (8). The calculated dependence of $V_z \, \mathrm{Rs}_d^{2/3}$ on $\Delta Z \equiv 1 - Z$ (where the estimation of Proposition 6, $C_1 \sim \mathrm{Rs}_d^{-2/3}$, is taken into account) is shown in Figure 4. The dependence is linear except for the buffer region near the orifice where the flow experiences rapid acceleration towards the draining pipe. Similar behaviour was observed in experiments carried out by Sakai et al. (1996). It can be noticed that the thickness of the buffer layer decreases slightly as Rs_d decreases. However, according to the analysis of Proposition 5, the buffer layer can not form an asymptotically thin boundary layer and the disturbances from the boundary conditions in the drain tend to propagate upstream.

The streamlines $\Psi = \mathrm{const}$ are shown in Figure 5 for different values of Rs_d and $L_d = 0.1$. Figure 5,b is plotted in logarithmic coordinates to demonstrate the slope of the streamlines which is found to be in a good agreement with the analysis of Proposition 6. If the intensity of vorticity is negligibly small, $\mathrm{Rs}_d = \infty$, then $\alpha = 2$. As Rs_d decreases, the region with $\alpha = 4/3$ is formed in the immediate vicinity of the axis while α remains equal to 2 in the other parts of the flow near the axis. Any further decrease of Rs_b causes broadening of the region with $\alpha = 4/3$ until the region of $\alpha = 2$ disappears. Then the region of $\alpha = 4/3$ starts to shrink into the region above the drain. The translational velocities near the drain and near the bottom of the tub remain relatively fast and neither the power-law approximation nor the strong vortex approximation are not valid in these regions. Convergence of the solution was not reached if Rs_d^2 is significantly smaller than 10. When local values of the Rossby numbers become too small, the flow looses its ability to adjust itself to the boundary conditions (Proposition 5) and be transformed into a pipe-type flow. We can expect that, under these conditions, the flow near the drain becomes fluctuating and most likely turbulent. According to equations (8) and (31) these disturbances would propagate upstream into the region above the drain.

The observed behaviour is determined by a relatively simple rule – the flow adjust itself to prevent the local Rossby number Rs_z being much smaller than 1. The dependence of C_1 evaluated in the region of $\alpha = 4/3$ on Rs_d is shown in Figure 6. This dependence matches well the estimates (34) of Proposition 6. The value of Rs_z^2 varies only slightly when Rs_d^2 changes several orders of magnitude. The weak dependence of Rs_z on Rs_d gives, however, a clear indication that Rs_z decreases when Rs_d decreases (near the axis the values of Rs_z and Rs are virtually the same). In the region of the 4/3 power-law, the value of Rs_z can be several orders of magnitude smaller than the global Rossby number Rs_d. Although in the presented calculations the local Rossby number does not, generally, reach very small values $\mathrm{Rs}_z \ll 1$, the strong vortex approximation appears to be applicable in quite a large region above the drain but not in the vicinity of the drain. As determined by equation (33), Rs_z increases towards the drain. The minimal local Rossby number at the drain orifice achieved in the calculations is $\mathrm{Rs}_z \approx 1$.

Besides the Rossby number, Rs_d, the flow in the near-axis region depends also on another dimensionless parameter, $L_d \equiv r_d/h$. In the strong vortex flow, the leading order representation of Ψ in (8) determines that $\partial^2\Psi/\partial Z^2 \approx 0$. Hence the parameter L_d does not affect the solution of equation (12) in this region. Since the translational velocities are fast and Rs_z is relatively large near the edge of the drain, the solution in this region is more affected by L_d. This behavior is illustrated in Figure 7 where the streamlines of two fields are shown for the same value of Rs_d and different values of L_d. In general, decreasing L_d does not make convergence of the solution more difficult although the precision of the finite difference approximation of the flow near the drain decreases. On the contrary, increasing L_d (while keeping Rs_d fixed) makes convergence either more difficult or impossible. This behaviour is in agreement with equation (28) of Proposition 2.

Under conditions discussed in Proposition 7, the 4/3 power-law region may extend far upstream from the drain. The region of $R/R_1 \sim 1$ is shown in Figure 8. The vertical line indicates the location of the R_1 specified by equation (35). This line represents the expected upstream boundary of the 4/3 power-law region. The power-law approximation is obviously not valid for any R near the bottom of the tank. A strong current towards the drain is formed there. It should be emphasized that this effect is not related to the viscous Ekman layer since viscosity is not considered in the present work. As it can be expected, the stronger vorticity in the flow extends the peripheral region further towards the axis.

7 Conclusions

Axisymmetric laminar flows in a bathtub with moderately high levels of vorticity and high values of the Reynolds numbers are considered. The drain radius r_d is assumed to be much smaller than the tub radius r_b. The flow is characterized by the geometry of the tub and by the Rossby number. Under normal conditions of existence of the bathtub vortex, the flow is divided into peripheral region which occupies most of the tub volume and the near-axis region. Since the flow characteristics of the peripheral region can be obtained easily, the focus of the present work is the flow in the near-axis region. While the overall Rossby number in the tub, Rs_b, can be small (small Rossby numbers correspond to relatively strong vorticity in the flow), the Rossby number characterizing the near-axis region $\mathrm{Rs}_d \sim \mathrm{Rs}_b(r_b/r_d)^2$ is much larger than Rs_b. The flow in the near-axis region is characterized by a slow temporal evolution but it can not be treated as a steady axisymmetric flow.

The major properties of the bathtub vortical flow are analyzed theoretically and numerically. Both analyses, theoretical and numerical, are in good agreement. The major results of the present work are:

1) Generally, if Rs_d is large the flow image on the radial-axial plane is close to the image of a potential flow. However, the local flow characteristics are determined by the local Rossby number, Rs, which can vary significantly in different parts of the flow near the axis and may differ from Rs_d by several orders of magnitude. Specifically, the region of strong vorticity and $\mathrm{Rs} \sim 1$ is observed in the immediate vicinity of the axis even if Rs_d is quite large.

2) It is shown that if the values of the local Rossby number near the drain are too small, the flow would not be able to satisfy the conditions in the drain. Physically, we can expect that the flow at the drain orifice becomes unsteady and turbulent. The disturbances from the drain are likely to propagate upsrteam.

3) It is shown that, if Rs_d is sufficiently small, the strong vortex approximation is applicable in a large region adjoint to the axis but not near the drain. The drain orifice is surrounded by the

buffer region where the flow goes through rapid acceleration towards the drain. Similar behaviour is observed in bathtub vortex experiments (Sakai et al. 1996).

4) When Rs_d is changed several orders of magnitude, the order Rs in the regions of strong vorticity is preserved.

5) The power-law representation of the stream function $\Delta\Psi \sim R^\alpha \Delta Z$ is valid in a large region near the axis but not in the vicinity of the drain and the bottom of the tub. Low levels of vorticity correspond to $\alpha = 2$ while high levels of vorticity correspond to $\alpha = 4/3$.

6) The numerical solutions obtained in the present work are, generally, stable when evolve temporally. However, even small deviations from the initial conditions used here may cause appearance of local recirculation zones that follow by rapid development of instabilities. No convergence was reached for Rs_d is significantly smaller than in the calculations presented. Although the geometric parameter $L_d \equiv r_d/h$ has much less effect on calculations than Rs_d, the convergence of the solutions is more difficult for smaller depth h.

Acknowledgment

The author thanks Prof. R. Fernandez-Feria for useful comments. This work is supported by Australian Research Council and The University of Queensland research grants.

References

Batchelor, G.: 1967, *An Introduction to Fluid Dynamics*, Cambridge University Press.

Einstein, H. and Li, H.: 1951, Steady vortex flow in a real fluid, *Proc. Heat Trans. and Fluid Mech. Inst.* **4**, 33–42.

Forbes, L. and Hocking, G.: 1994, The bath-plug vortex, *J.Fluid Mech.* **284**, 43–62.

Greenspan, H.: 1968, *The theory of rotating fluids*, Cambridge University Press.

Klimenko, A.: 1998a, Conditional methods in application for Lagrangian modelling, *Physics of Fluids* **10**, 922–927.

Klimenko, A.: 1998b, Evolution of vorticity in the bathtub vortex, *13th Australasian Fluid Mechanics Conference*, Vol. 2, pp. 781–784.

Lewellen, W.: 1962, A solution for three-dimensional vortex flows with strong circulation, *J.Fluid Mech.* **14**, 420–432.

Long, R.: 1953, Steady motion around a symmetrical obstacle moving along the axis of a rotating fluid, *Journal of Meteorology* **10**, 197–203.

Lundgren, T.: 1985, The vortical flow above the drain-hole in a rotating vessel, *J.Fluid Mech.* **155**, 381–412.

Marris, A.: 1967, Theory of the bathtub vortex, *Journal of Applied Mechanics* **61**, 11–15.

Sakai, S., Madarame, H. and Okamoto, K.: 1996, Gas core shape and velocity distribution around a bathtub vortex, *ASME Fluids Eng. Division Conference*, Vol. 3, pp. 113–120.

Shapiro, A.: 1962, Bath-tub vortex, *NATURE* **196**, 1080–1081.

Vanyo, J.: 1993, *Rotating fluids in Engineering and Science*, Butterworth - Heinemann.

Figure Captures

Figure 1. Schematic of the bathtub flow.

Figure 2. The calculation domain and the boundary conditions.

Figure 3. Vorticity evolution in a bathtub-type flow.

Figure 4. The normalized axial velocity $V_z \, \mathrm{Rs}_d^{2/3}$ as a function of $\Delta Z = 1 - Z$ for $R = \{0.04,\ 0.18,\ 0.32,\ 0.47\}$. Smaller values of V_z correspond to larger R.

Figure 5. The streamlines $\Psi = \mathrm{const}$ for $L_d = 0.1$ and several values of the parameter Rs_d plotted using a) the conventional coordinates and b) the logarithmic coordinates.

Figure 6. The calculated values of C_1 as a function of Rs_d^2.

Figure 7. The streamlines $\Psi = \mathrm{const}$ for $\mathrm{Rs}_d^2 = 10$ and different values of the parameter L_d.

Figure 8. The streamlines $\Psi = \mathrm{const}$ in the region $R/R_1 \sim 1$ of the vortical flow with $\mathrm{Rs}_d^2 = 50$ and $L_d = 0.01$ plotted in logarithmic coordinates. The figure in the corner is the same but plotted using the conventional coordinates.

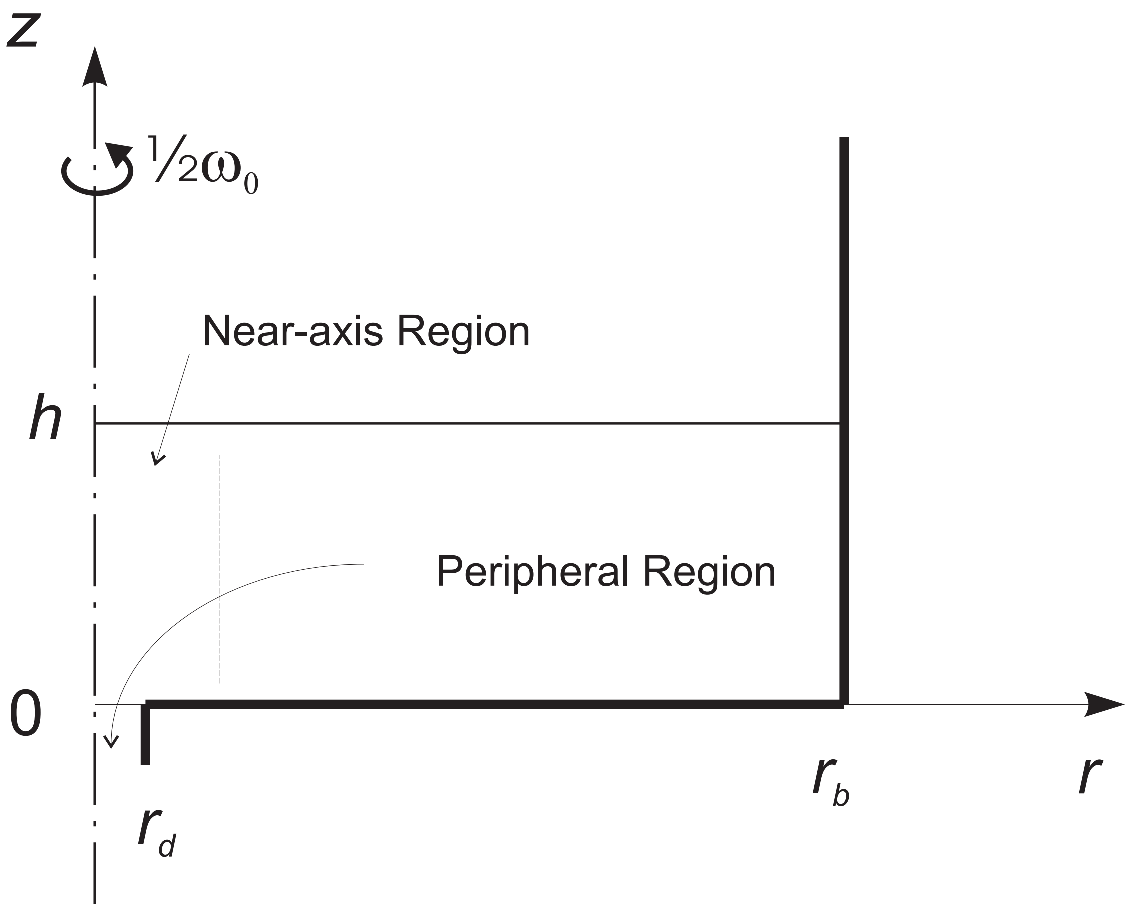

z
½ω0
Near-axis Region
h
Peripheral Region
0
rd
rb
r

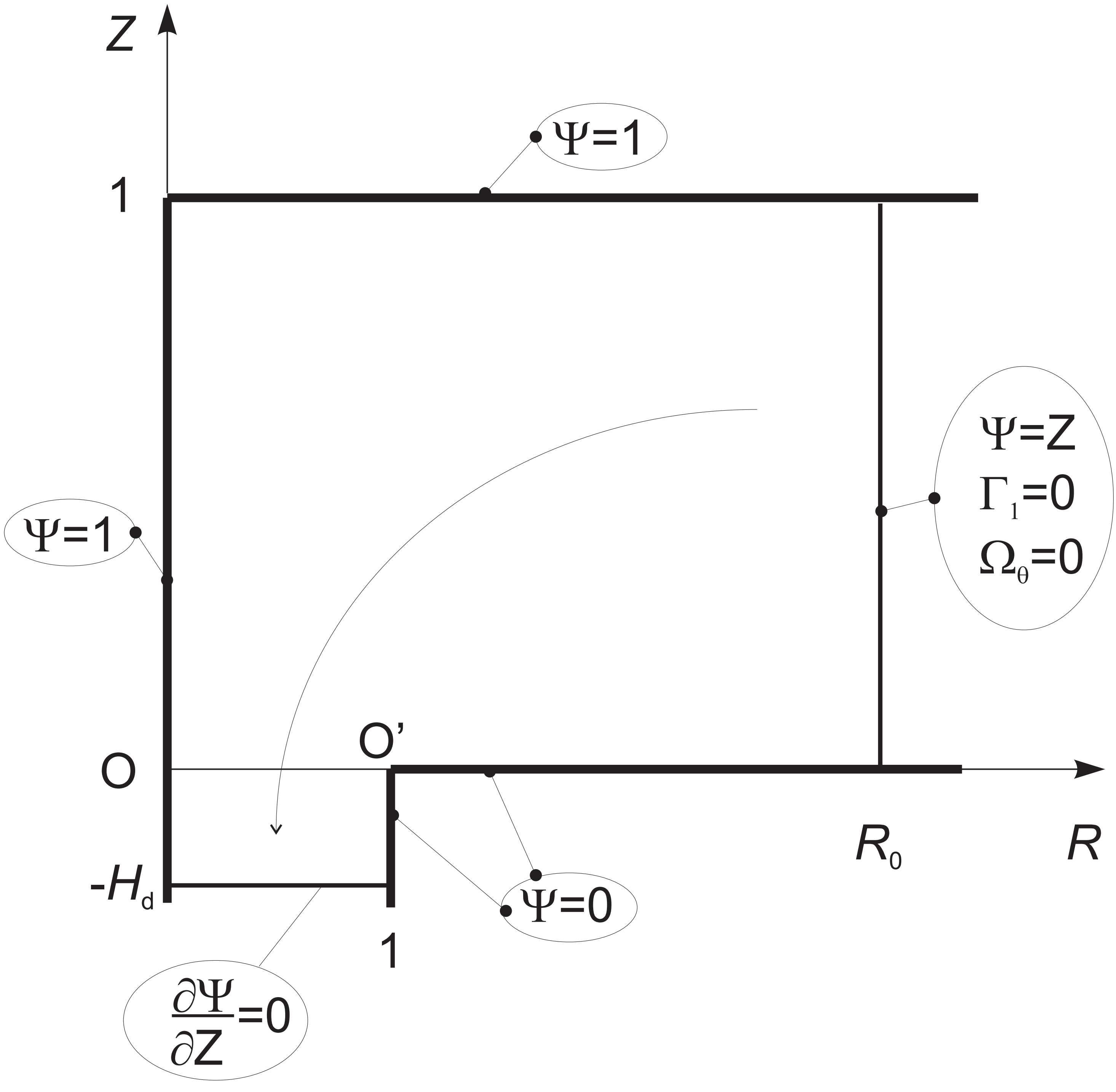

Z
Ψ=1
1
Ψ=Z
Γ_1=0
Ω_θ=0
Ψ=1
O'
O
R_0
R
$-H_d$
Ψ=0
1
$\frac{\partial\Psi}{\partial Z}$=0

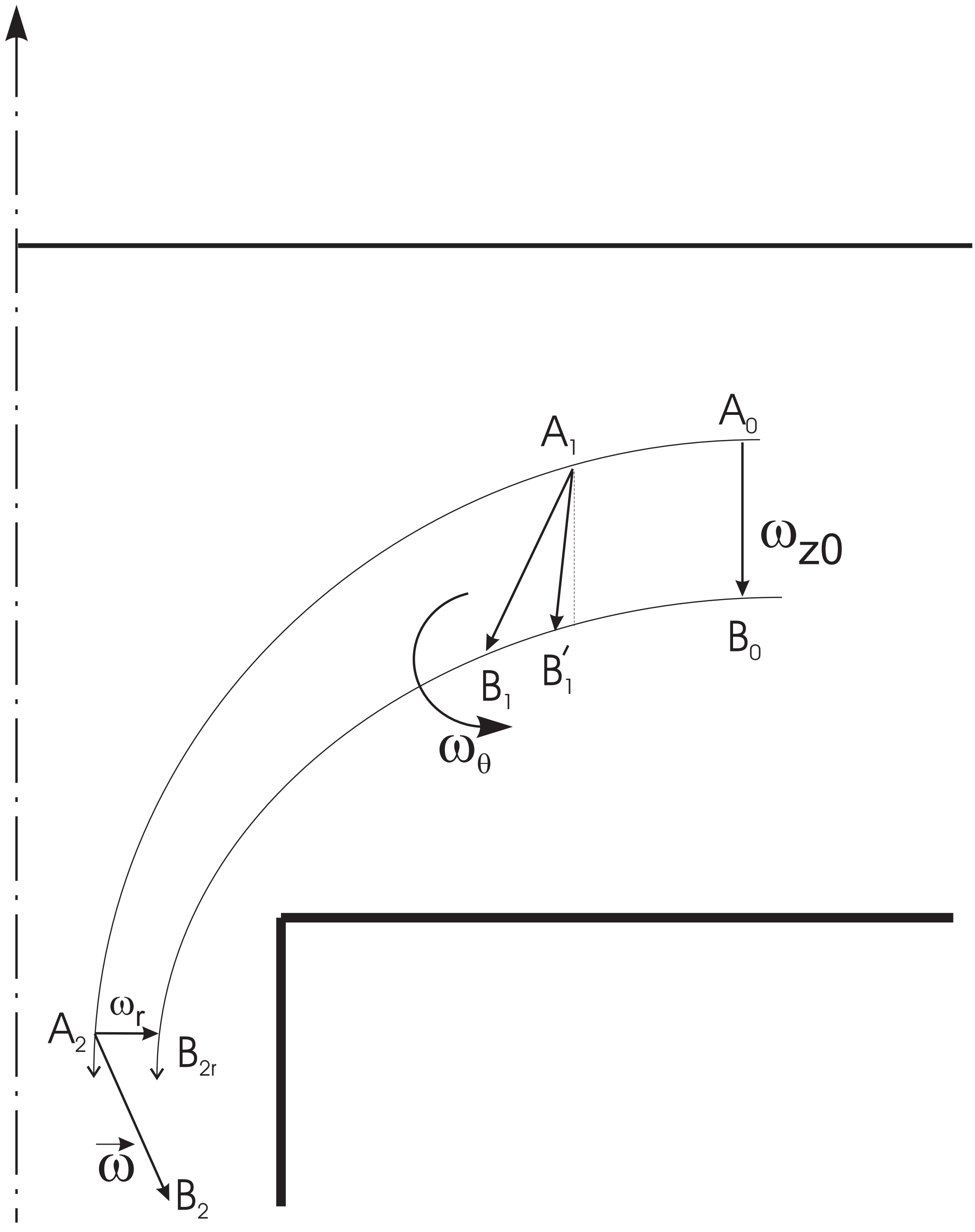

A1
A0
ωz0
B'1
B1
B0
ωθ
A2
ωr
B2r
ω
B2

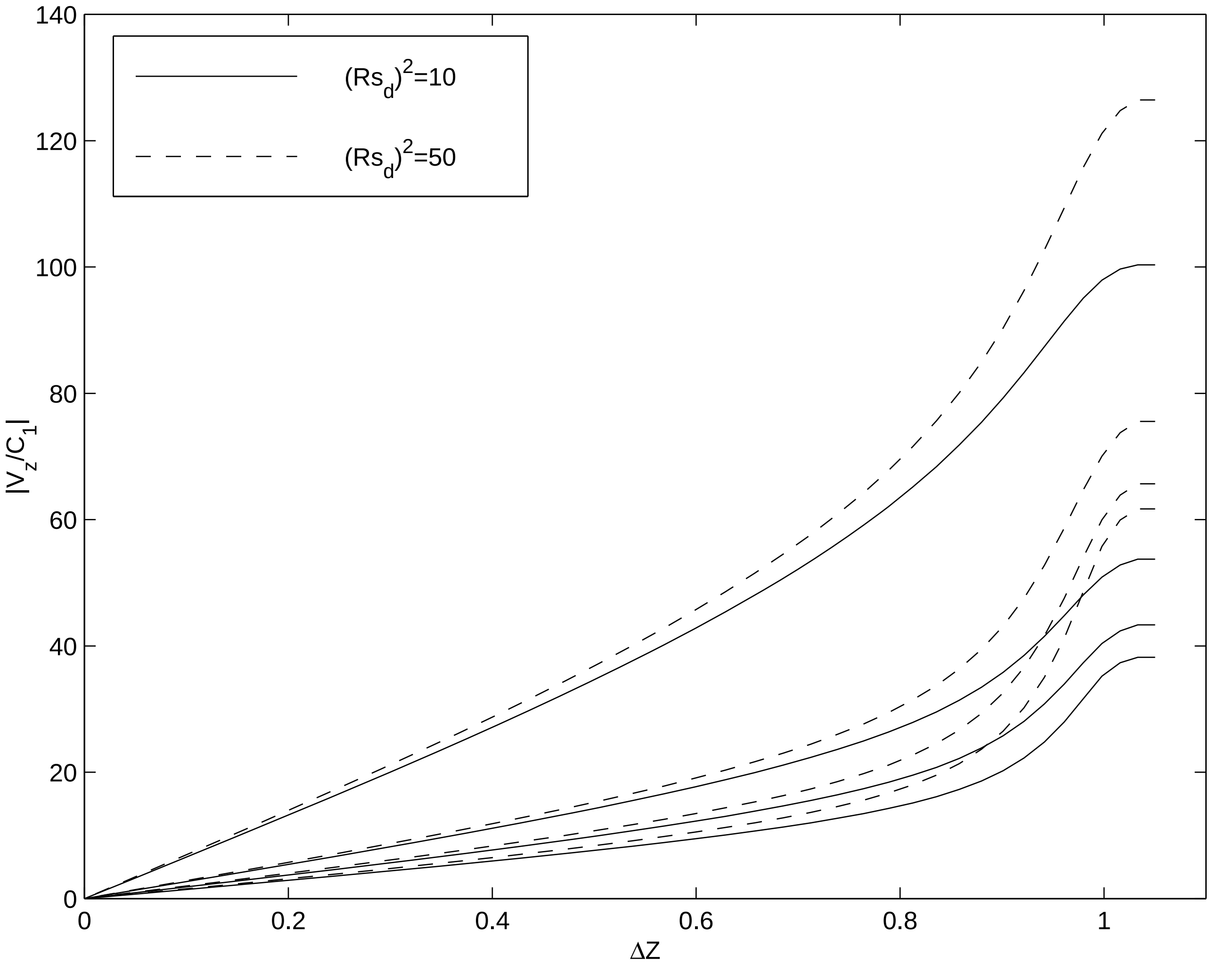

140
120
100
80
60
40
20
0
0
0.2
0.4
0.6
0.8
1
ΔZ
$|V_z/C_1|$
$(Rs_d)^2$=10
$(Rs_d)^2$=50

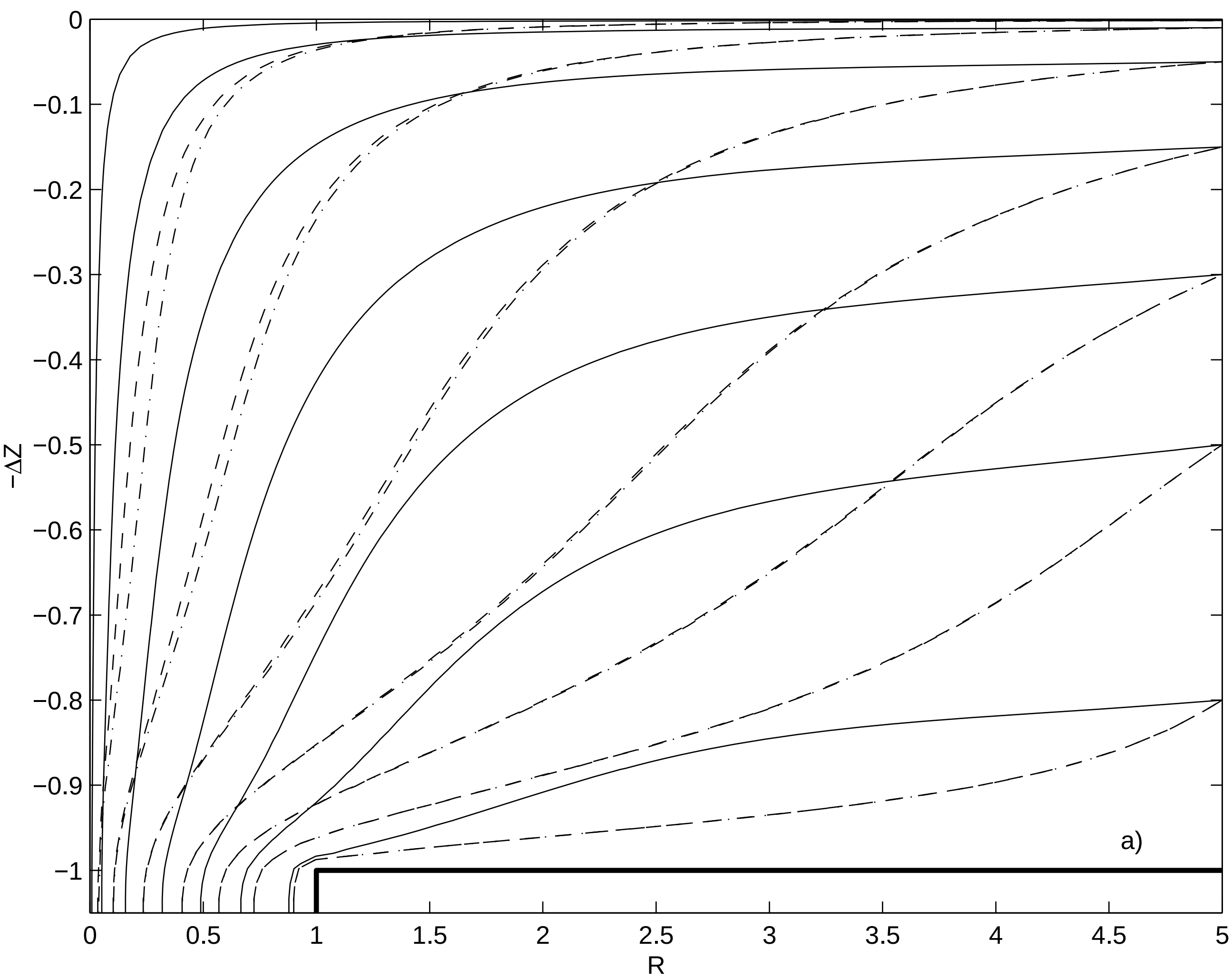
0
−0.1
−0.2
−0.3
−0.4
−0.5
−0.6
−0.7
−0.8
−0.9
−1
−ΔZ
0
0.5
1
1.5
2
2.5
3
3.5
4
4.5
5
R
a)

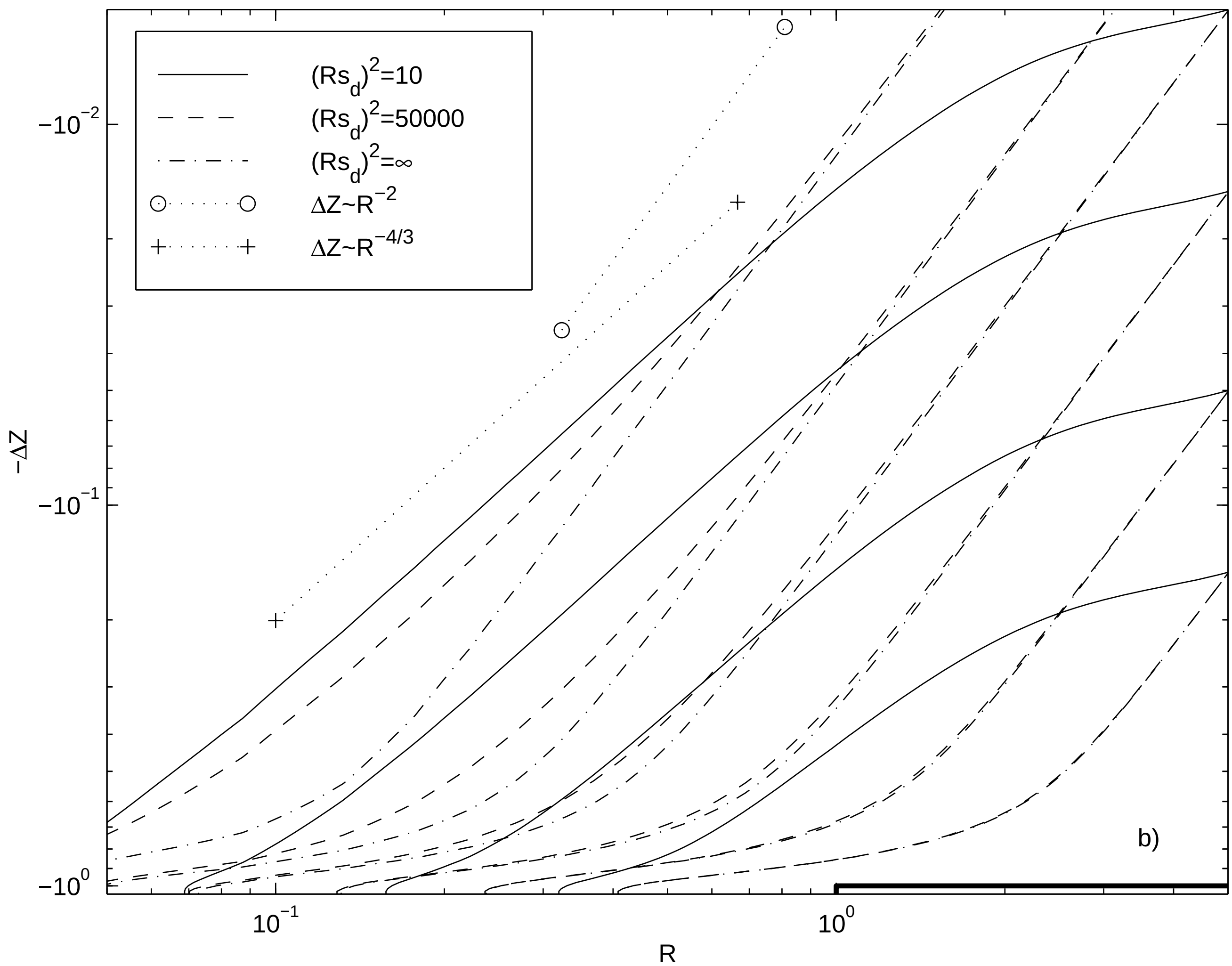

$(Rs_d)^2$=10
$(Rs_d)^2$=50000
$(Rs_d)^2$=∞
ΔZ~R^{-2}
ΔZ~R$^{-4/3}$
−10^{-2}
−10^{-1}
−10^{0}
−ΔZ
10^{-1}
10^{0}
R
b)

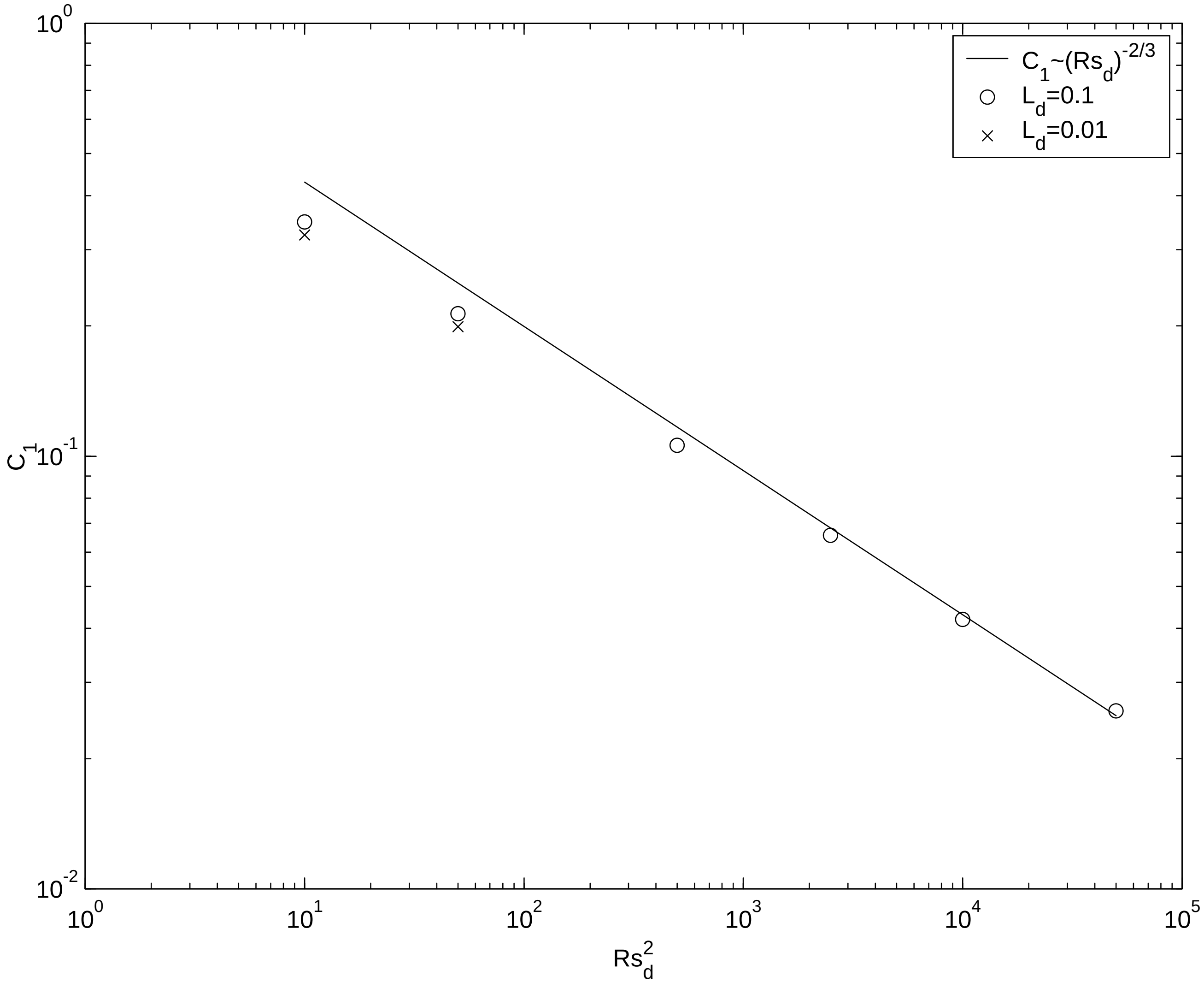

$C_1 \sim (Rs_d)^{-2/3}$
$L_d=0.1$
$L_d=0.01$
10^0
10^{-1}
10^{-2}
C_1
10^0
10^1
10^2
10^3
10^4
10^5
Rs_d^2

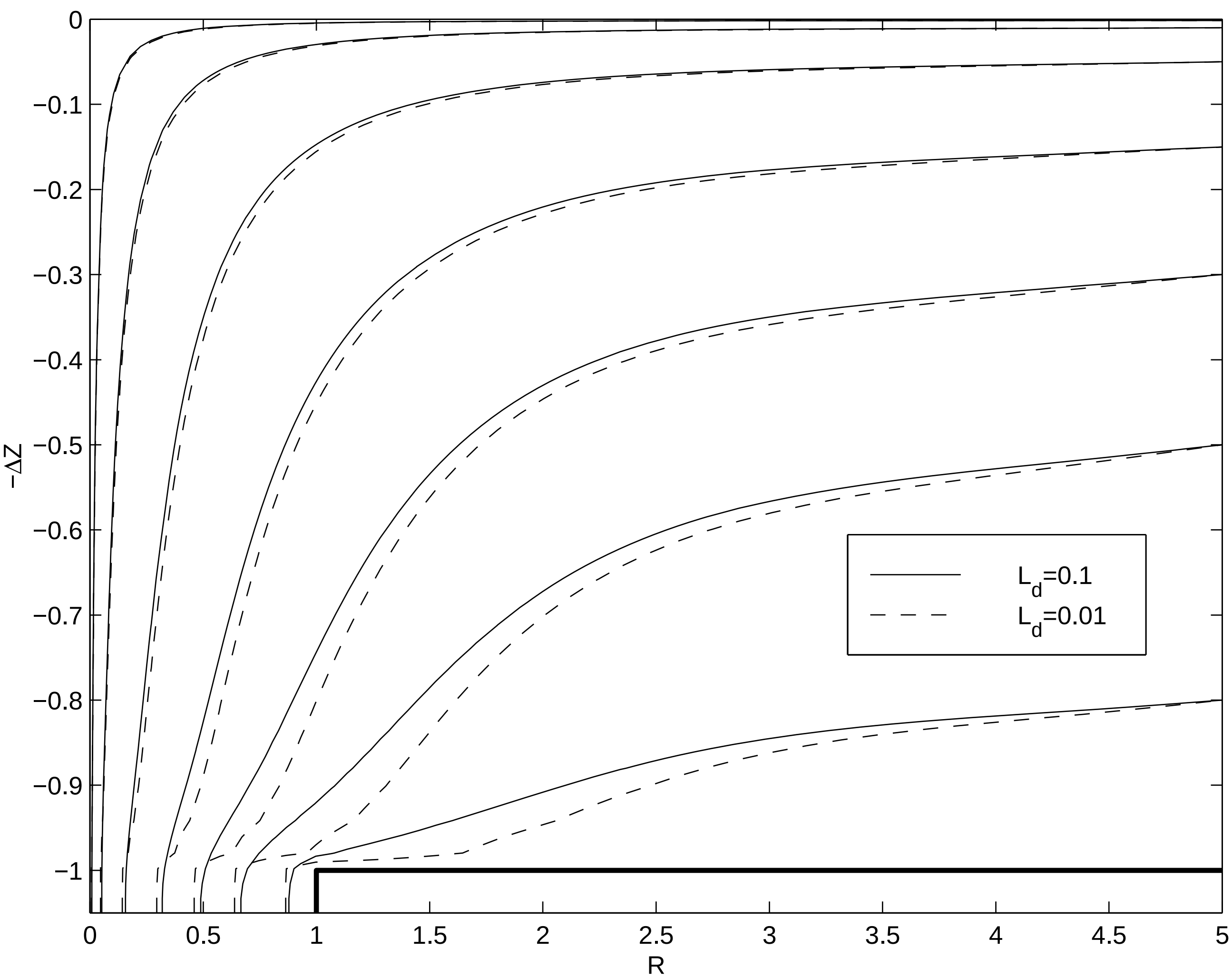

0
−0.1
−0.2
−0.3
−0.4
−0.5
−0.6
−0.7
−0.8
−0.9
−1
−ΔZ
0
0.5
1
1.5
2
2.5
3
3.5
4
4.5
5
R
L_d=0.1
L_d=0.01

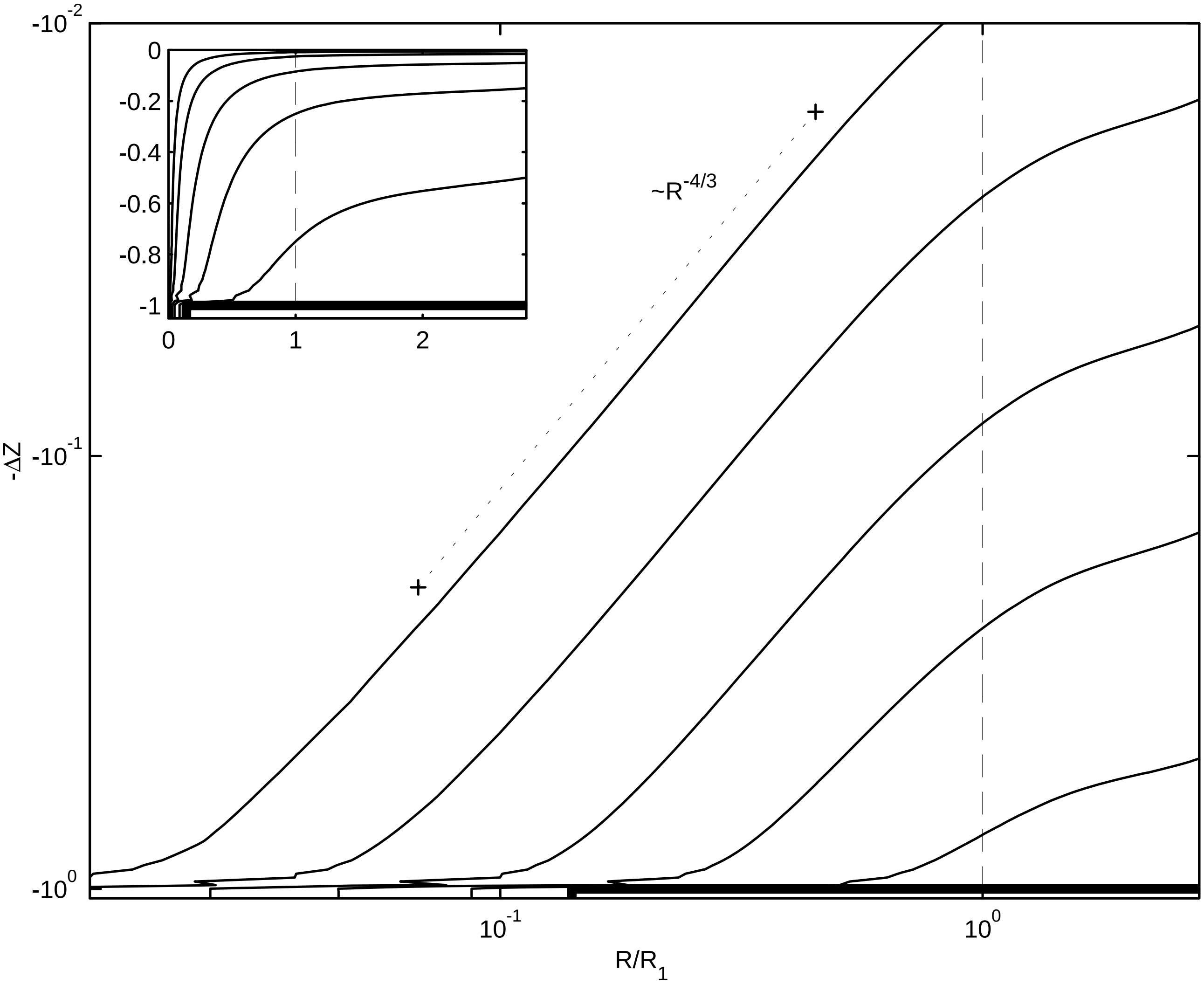

-10^-2
-10^-1
-10^0
-ΔZ
10^-1
10^0
R/R_1
~R^-4/3
0
-0.2
-0.4
-0.6
-0.8
-1
0
1
2